PERGAMON

Organic Geochemistry 30 (1999) 1559–1569

Organic Geochemistry

www.elsevier.nl/locate/orggeochem

Detection of petroleum contamination in river sediments from Quebec City region using GC–IRMS

K.M. Rogers [a,*], M.M. Savard [b]

[a] *Institute of Geological and Nuclear Sciences, PO Box 31-312, Lower Hutt, New Zealand*
[b] *Delta Lab, GSC-Québec, Centre Géoscientifique de Québec, 2700 rue Einstein, CP 7500, Ste-Foy, Quebec, Canada G1V 4C7*

Received 5 June 1998; accepted 31 August 1999
(returned to author for revision 27 December 1998)

Abstract

Isotopic analysis by compound specific gas chromatography–isotope ratio mass spectrometry (GC–IRMS) is used to detect and characterize petroleum pollution in surficial sediments along the St Lawrence River, near Quebec City. Unusually mature *n*-alkane distributions have been found in some recent intertidal sediments in the region. GC–IRMS results suggest that the *n*-alkanes are not derived from indigenous organic sources because they carry $\delta^{13}C$ values between −30.0 and −27.0‰, as well as very small isotopic differences between odd and even numbered *n*-alkanes, which are both typically associated with petroleum products. Comparison of these sediments with bunker fuel, an oil used in the shipping industry, has shown a close isotopic correlation in some sites, which is further supported by biomarkers. Overall, the contamination has been dispersed along the river but is generally localized around the industrial region where hydrocarbon transfer from shore storage to ships takes place. This study illustrates how GC–IRMS can be used effectively in the detection and characterization of petroleum pollutants in sediments.

Keywords: Hydrocarbon pollution; *n*-Alkanes; GC–IRMS; GC–MS; Stable carbon isotopes

1. Introduction

Continuous flow isotope analysis [gas chromatography–isotope ratio mass spectrometry (GC–IRMS)] has not been extensively used in environmental studies of sedimentary hydrocarbon contaminants. In uncontaminated sediments, *n*-alkanes arise primarily from autochthonous organic material. Marine organisms synthesize preferentially short-chain, odd carbon-numbered *n*-alkanes such as C_{15} and C_{17} (Clark and Blumer, 1967; Gelpi et al., 1970; Blumer et al., 1971). Terrestrial higher plants usually contain long-chain, odd carbon-numbered *n*-alkanes ranging from C_{25} to C_{33} (Eglinton et al., 1962; Simoneit, 1978). More recently, Lichtfouse et al. (1994) suggest possible algal origins of long-chain odd-numbered *n*-alkanes. In contrast, anthropogenic sources such as petroleum products may exhibit either long- or short-chain *n*-alkanes depending on source, but usually with almost equal amounts of even and odd carbon-numbered *n*-alkanes.

Varying source inputs and/or biodegradation can alter sedimentary *n*-alkanes resulting in bimodal or reduced distributions, which do not accurately reflect source input. Continuous flow GC–IRMS permits isotopic characterization and comparison of individual *n*-alkane components, therefore allowing the source to be determined more accurately.

Previous investigations of $\delta^{13}C$ values for individual organic compounds can serve for comparative purposes. Rieley et al. (1991) isotopically characterized odd carbon-numbered C_{25-33} *n*-alkanes from lake sediments

* Corresponding author. Tel.: +64-4-5704636; fax: +64-4-5704657.
E-mail address: k.rogers@gns.cri.nz (K.M. Rogers).

0146-6380/99/$ - see front matter
PII: S0146-6380(99)00132-1

and leaf waxes. $\delta^{13}C$ values ranged from −35.9 to −30.1‰ and −38.7 to −30.1‰ for the lake sediments and leaf waxes, respectively. Harada et al. (1995) suggested isotopic signals between −22.0 and −18.0‰ for recent marine-derived organic carbon. Modern C_3 plants range from −23 to −34‰ (Rieley et al., 1991), while Collister et al. (1994) reported *n*-alkane isotopic values between −28.5 and −26.0‰ from modern C_4 plants. Uzaki et al. (1993) and Ishiwatari et al. (1994) studied surface samples in Tokyo Bay and gave the isotopic range of hydrocarbon pollution from −31.5 to −28.2‰ using C_{27-33} *n*-alkanes.

Effects of biodegradation on individual compounds have been previously investigated. Sofer et al. (1991) and Mansuy et al. (1996) suggested that the isotopic composition of *n*-alkanes, measured using continuous flow GC–IRMS between nC_{12} and nC_{32}, is not affected by biodegradation or maturity. However, Boreham et al. (1994) and Collister et al. (1994) observed changes in the isotopic profiles during artificial maturation of lacustrine kerogens, while Hirner and Lyon (1989) found that biodegradation of saturates (specifically the *n*-alkanes) and aromatics resulted in slightly heavier bulk isotopic compositions. Therefore, GC–IRMS could be a useful analytical tool for samples that show slight to moderately biodegraded *n*-alkane patterns or multiple source inputs.

An isotopic study of individual *n*-alkanes in recent river sediments from the St Lawrence River, Quebec City, Canada, is used to identify hydrocarbon contamination in the region. The river is a major waterway for the shipping industry, as well as a popular recreational site for the general public and, therefore, several sources of contamination may be possible. One of the most common petroleum products used by the local shipping industry is bunker fuel, which is used as a boiler fuel in ships and for industrial heating. It is a viscous fluid with a hydrocarbon range from C_9 to C_{36} (Kaplan et al., 1996).

The objectives of this study were to evaluate the potential of GC–IRMS as an environmental research tool, and to understand the distribution of hydrocarbon pollution along the St Lawrence River near Quebec City.

2. Experimental

2.1. Samples

Recent surface (0–10 cm) and subsurface (10–20, 20–30, and 30–40 cm) samples were taken from the intertidal zone of the St Lawrence River from different locations near Quebec City (Fig. 1). The samples consisted of coarse beach sand which were hand-picked to remove large stones and organic debris, washed with distilled water, air dried, and refrigerated until analysis. In most cases, volatiles (C_{4-10} homologues) had already evaporated from the samples before collection. It has been determined that evaporation during storage does not result in isotopic fractionation of light hydrocarbons (Bjorøy et al., 1994).

The river is influenced by tides and strong currents that flow predominantly west to east towards the Atlantic Ocean, thus permitting dispersal of any spillage over a wide area. In the study area (Fig. 1) there are two hydrocarbon transfer stations between ship and shore at Sites 1 and 3, close to Quebec City. Samples were selected from the intertidal beaches surrounding these stations, along with samples from Sites 2 and 2a (located adjacent to a petroleum storage site which is undergoing an environmental cleanup process). Sites 4 and 5 were located furthermost west and east from the hydrocarbon storage sites and were least likely to be affected by contamination. They were sampled to examine the lateral and regional distribution of anthropogenic input along the river. A fresh sample of bunker fuel was also used for comparative purposes, as it is one of the principal fuels used by ships on the river.

2.2. Sample preparation and analysis

Pyrolysis was used to determine the total organic content of each sample. Beach sand from the river was air dried, then a 5g portion was placed in a porcelain crucible, heated in a furnace at 400°C for 4 h, then cooled to room temperature in a desiccator. Organic content was calculated from the weight difference (±2 mg organics/g sediment).

The organic fraction was extracted from the bulk sample by ultrasonic agitation for 30 min with dichloromethane, and separated by filtration. The extract was concentrated by nitrogen blow-down and asphaltenes precipitated with *n*-hexane. Purification of the saturate fraction was carried out by column chromatography on a silica column, loaded with the extract and eluted with *n*-hexane. The fraction was not purified further as Collister et al. (1994) had previously showed that the $\delta^{13}C$ values of *n*-alkanes isolated by urea adduction was unchanged compared to *n*-alkanes from the saturated hydrocarbon fraction. To monitor co-elution problems which may occur in the long-chain region of the chromatogram, some samples were treated with urea and re-analysed. These samples were within the statistical errors. For comparative purposes, an aliquot of Bunker fuel oil was processed in a similar manner as the organic extracts.

GC of C_{11-30} *n*-alkanes was conducted on a Hewlett Packard model 5890 series II gas chromatograph fitted with a CP Sil-5CB fused silica capillary column (25 m× 0.25 mm i.d.×0.25 μm film thickness). The oven was programmed from 40°C (1 min) to 120°C at 30°C min^{-1}, then to 290°C (30 min) at 2°C min^{-1}. Selected ratios of the *n*-alkanes were calculated using peak area integration.

GC–MS analyses were performed using a Hewlett Packard 5995C system with a J&W DB-1 (30 m×0.2 mm

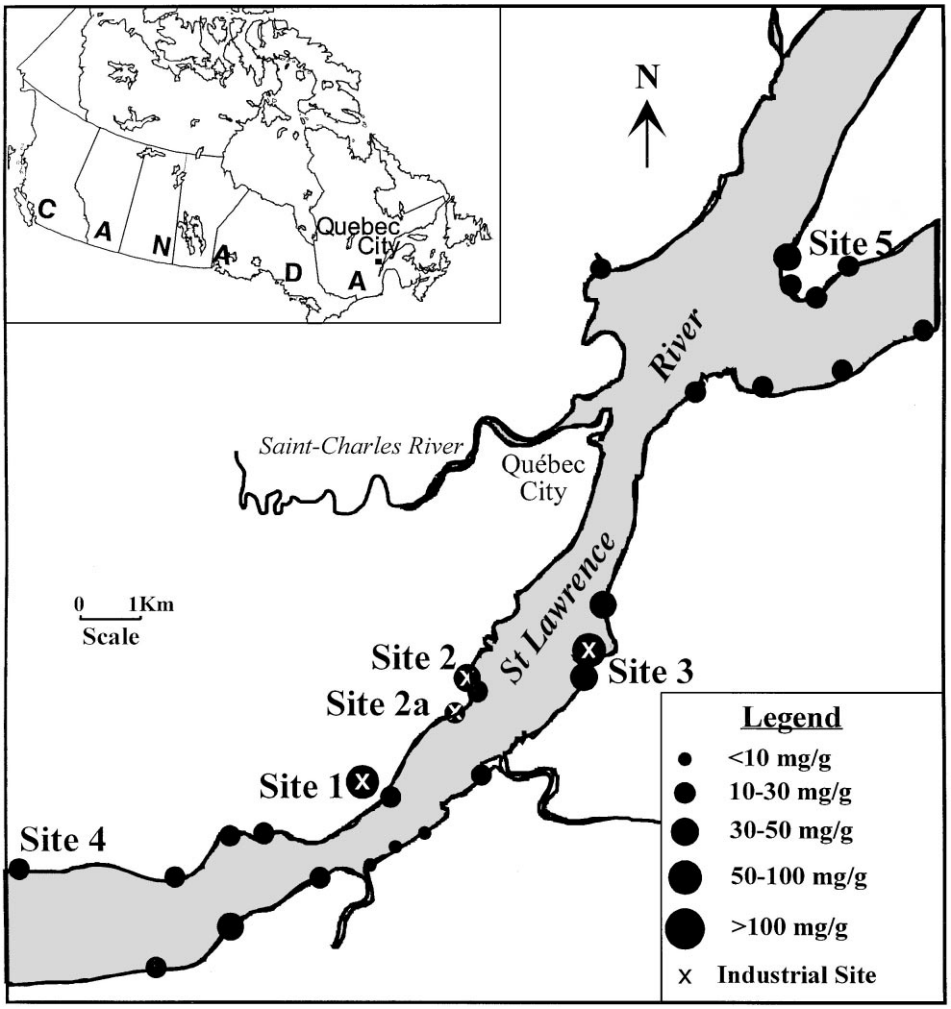

Fig. 1. Location of sample sites and relative contamination levels (mg hydrocarbons/g sediment) in the St Lawrence River.

i.d.×0.25 μm film thickness) fused silica column. The oven was programmed from 40°C (1 min) to 120°C at 30°C min^{-1}, then to 290°C (30 min) at 2°C min^{-1}. Peak identification (Table 1) was carried out using co-injected standards and retention times from previously identified oils.

Individual $\delta^{13}C$ *n*-alkane values were obtained using a VG PRISM III combined with a cupric oxide-packed ISOCHRON furnace combustion unit (850°C), and a Hewlett Packard model 5890 series II gas chromatograph. Samples were injected onto a HP Ultra 1 (cross-linked methyl siloxane) fused silica column (50 m×0.32 mm i.d.×0.52 μm film thickness) with splitless mode. The oven was programmed from 40°C (1 min) to 120°C at 20°C min^{-1}, then to 290°C (30 min) at 2°C min^{-1} using helium as carrier gas. An isotopically predetermined mixture comprising decane, undecane, dodecane and methyl-decanoate was used as an *n*-alkane standard before each run. A standardized cylinder of CO_2 gas was used to calibrate each sample with two pulses used before and after each run, as well as the use of an internal standard 5α-androstrane, eluting between nC_{20} and nC_{21}. All results are reported as per mil (‰) relative to a reference gas calibrated to the carbon isotopic composition of NBS-19 standard. Reproducibility of results was within 0.3‰ (1 σ_n) and for the standards, better than 0.1% (standard deviation).

3. Results

3.1. Organic extraction and pyrolysis

The organic extracts from the various sands ranged from a slight, pale yellow residue to a thick, dark petroleum-like product, similar in characteristics to

bunker fuel. Pyrolysis of the samples determined their relative organic contents, which varied from around 10 mg organic matter/g sediment to 130 mg organic matter/g sediment (Fig. 1). Areas with higher organic content levels were those adjacent to petroleum storage sites (Sites 1, 2, and 3, between 30 and 133 mg/g). The organic content diminished further towards the east (Site 5, between 10 and 25 mg/g) and west (Site 4, between 9 and 17 mg/g). The highest organic content (133 mg/g) was sampled from a drainage area adjacent to an industrial petroleum storage area (Site 1).

Table 1
Terpane and sterane peak identification

Peak	Description	Carbon no.
Steranes		
1	13β(H), 17α(H)-Diacholestane (20S)	27
2	13β(H), 17α(H)-Diacholestane (20R)	27
3	5α(H), 14α(H), 17α(H)-Cholestane (20R)	27
4	24-Methyl-5α(H), 14α(H), 17α(H)-cholestane (20R)	28
5	24-Ethyl-5α(H), 14α(H), 17α(H)-cholestane (20S)	29
6	24-Ethyl-5α(H), 14β(H), 17β(H)-cholestane (20R)	29
7	24-Ethyl-5α(H), 14β(H), 17β(H)-cholestane (20S)	29
8	24-Ethyl-5α(H), 14α(H), 17α(H)-cholestane (20R)	29
9	24-Propyl-5α(H), 14α(H), 17α(H)-cholestane (20S)	30
10	24-Propyl-5α(H), 14β(H), 17β(H)-cholestane (20R)	30
11	24-Propyl-5α(H), 14β(H), 17β(H)-cholestane (20S)	30
12	24-Propyl-5α(H), 14α(H), 17α(H)-cholestane (20R)	30
Terpanes		
a	18α(H)-22,29,30-Trisnorneohopane (Ts)	27
b	17α(H)-22,29,30-Trisnorhopane (Tm)	27
c	17α(H), 21β(H)-30-Norhopane	29
d	17β(H),21α(H)-30-Norhopane (normoretane)	29
e	17α(H), 21β(H)-Hopane	30
f	17β(H),21α(H)-Moretane	30
g,h	17α(H), 21β(H)-30-Homohopane (22S, 22R)	31
i,j	17α(H), 21β(H)-30,31-Bishomohopane (22S,22R)	32
k,l	17α(H), 21β(H)-30,31-32-Trishomohopane (22S, 22R)	33
m	17α(H), 21β(H)-20,30-Bisnorhopane	28
n	17β(H)-22,29,30-Trisnorhopane	27
0	18α-(H)Oleanane	30

3.2. GC

The *n*-alkane distributions of the saturate fractions are generally unimodal (between C_{11} and C_{31}), with a maximum at nC_{15} or nC_{17}, although a slight bimodal distribution at nC_{29} was seen at Site 4. Carbon preference index values ($CPI_{15–21}$ and $CPI_{25–31}$) were compared to investigate the main *n*-alkane source distribution from higher and lower molecular weight *n*-alkanes (Table 2).

Surface samples (0–10 cm) from Sites 1, 2, and 3 contained $CPI_{15–21}$ values around unity, whereas the $CPI_{25–33}$ values were generally higher. Subsurface samples (between 10 and 40 cm) from Sites 1, 2, and 3 showed that $CPI_{15–21}$ values were approximately at unity (0.97–1.09), but the $CPI_{25–31}$ values of the same samples were slightly higher (up to 1.46).

Surface samples (0–10 cm) located further away from the central industrial region (Sites 4 and 5) showed higher $CPI_{15–21}$ values than for surface samples located closer to the industrial sites (Sites 1, 2, and 3). The $CPI_{25–31}$ values from Sites 4 and 5 were also higher than corresponding $CPI_{15–21}$ values from these sites, and the $CPI_{25–31}$ values from Sites 1, 2, and 3.

3.3. GC–MS

Triterpane and sterane biomarker ratios of sediments were used to examine their overall maturity (Fig. 2,

Table 2
Carbon preference index (CPIs) of surface and sub-surface samples from the St Lawrence River

Site	Depth (cm)	Pr/nC_{17}	$CPI_{15–21}$	$CPI_{25–33}$
1	0–10	1.52	1.37	1.33
	0–10	1.39	0.87	0.94
	0–20	0.90	1.03	1.38
	20–30	0.93	0.93	1.38
	30–40	0.43	0.99	1.46
	30–40	0.38	1.04	0.89
2	0–10	1.32	0.91	1.07
	0–10	0.95	1.17	0.82
	0–10	1.00	0.77	0.94
	10–20	0.78	1.06	0.79
	30–40	0.41	1.07	1.26
2a	Contaminated	1.53	0.97	nd[a]
	0–10	1.87	0.87	1.73
	0–10	2.42	0.97	1.56
3	0–10	0.50	1.14	1.56
4	0–10	0.88	1.20	1.65
	10–20	0.63	1.34	1.76
5	0–10	2.22	0.61	1.07
	0–10	0.65	1.18	1.54
Bunker fuel		0.97	1.02	nd

[a] nd = not detected.

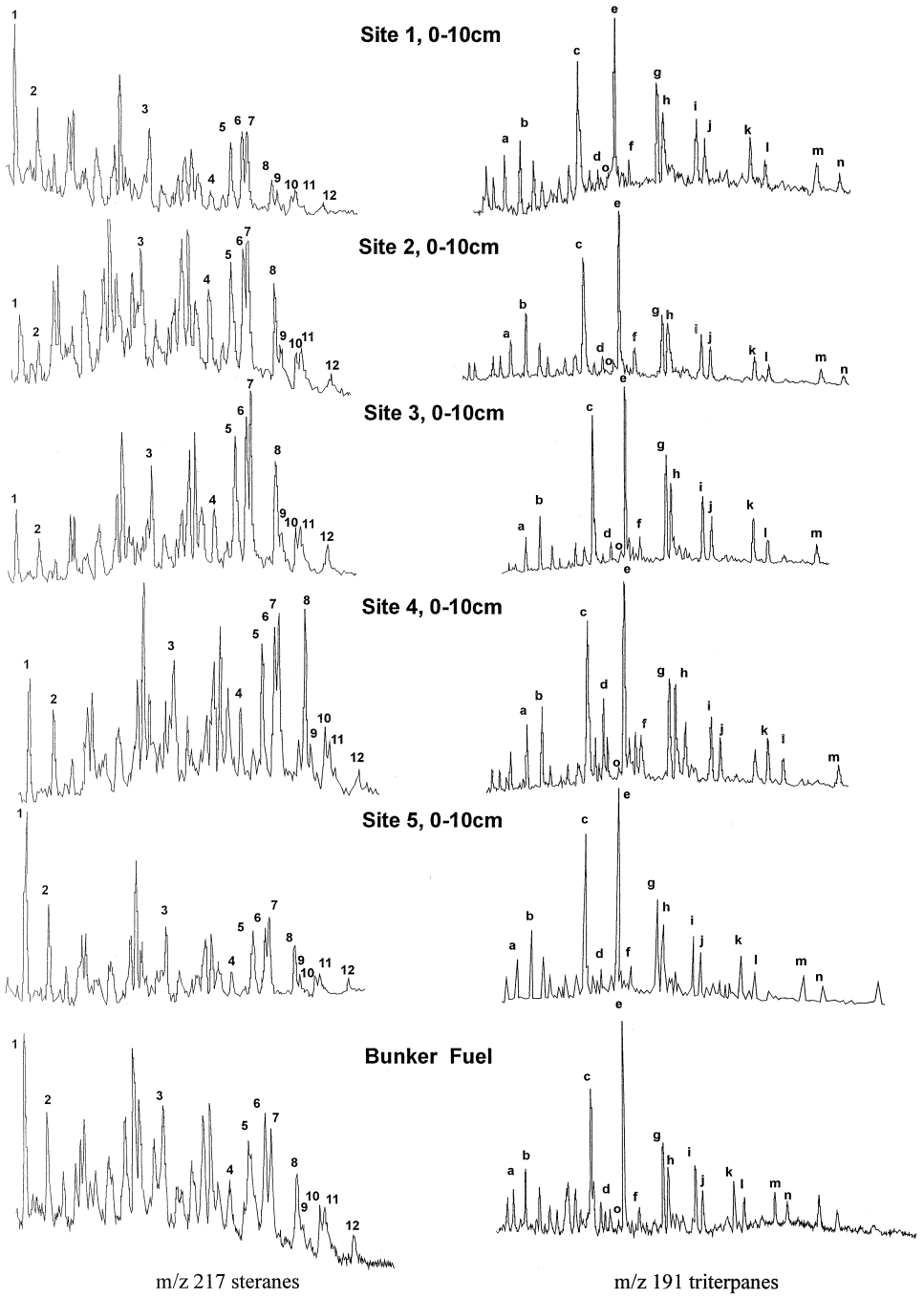

Fig. 2. Triterpane and sterane chromatograms of sediment samples and bunker fuel. Samples 8 and 6 are from Site 1, Sample 10 from Site 2a, Sample 20 from Site 3, Sample 24 from Site 4, and Sample 23 from Site 5.

Tables 3 and 4). These were also compared to Bunker fuel, as it was the main suspected contaminant in the region. Biomarkers are much less susceptible to biodegradation than *n*-alkanes and isoprenoid hydrocarbons (Volkman, 1984) thus can be used reliably for source identification and thermal maturity parameters. Because of extensive biodegradation, *n*-alkanes had been removed from Sample 8, Site 1, but this sample could still be characterized using GC–MS.

In general, triterpane 'fingerprints' (as evidenced by m/z 191 mass chromatograms, Fig. 2) are similar to each other and dominated by the $C_{29}17\alpha$(H)-norhopane and

Table 3
Terpane biomarker ratios

Sample	Ts (Ts + Tm)	C_{29} moretane C_{29} hopane	C_{30} moretane C_{30} hopane	C_{31}S/S + R homohopane	C_{29} morhopane C_{30} hopane	Oleanane C_{30} hopane
Site 1 (0–10 cm)	0.61	0.28	0.33	0.52	0.81	0.13
Site 2a (0–10 cm)	0.55	0.20	0.19	0.54	0.84	0.14
Site 2 (0–10 cm)	0.64	0.18	0.21	0.55	0.79	0.12
Site 3 (0–10 cm)	0.62	0.14	0.17	0.56	0.76	0.13
Site 4 (0–10 cm)	0.55	0.49	0.39	0.42	0.85	0.07
Site 5 (0–10 cm)	0.52	0.14	0.13	0.47	0.78	0.07
Bunker fuel	0.60	0.07	0.16	0.54	0.75	0.13

$C_{30}17\alpha$(H)-hopane, with a smooth decrease in the abundance of $C_{31–35}$ homohopanes (Fig. 2). Triterpane ratios were fairly uniform between Sites 1, 2, and 3; (Ts/Ts + Tm) between 0.52 and 0.64; (C_{29} norhopane/C_{30} hopane) between 0.76 and 0.89; (oleanane/C_{29} norhopane) between 0.07 and 0.14; and (C_{31} homohopane S/S + R) between 0.42 and 0.56 (Table 2). C_{29}Ts and other diahopanes are present in all the samples. The sample from Site 4 contains the highest C_{29} and C_{30} moretane/hopane ratios of 0.49 and 0.39, respectively, and the lowest C_{31} homohopane S/S + R ratio of 0.42.

Sterane distributions and maturity parameters are shown in Table 4. The samples from Sites 1, 2, and 3 display similar sterane 'fingerprints' (m/z 217 mass chromatograms; Fig. 2) and have the highest maturity level. The sterane pattern shows relatively equal quantities of C_{27} and C_{29} components (between 30 and 40‰, respectively), slightly lower C_{28} steranes (approx. 25%) and a minor C_{30} sterane contribution (between 4.0 and 9.4%) in all samples. Maturity parameters based on steranes such as %ββ C_{29} and C_{27} steranes show only minor variations between Sites 1, 2, and 3 and suggest little or no autochthonous contribution.

3.4. GC–IRMS

The isotopic values of *n*-alkanes between C_{11} and C_{31} of all sites are presented in Table 5. Surface samples (0–10 cm) were compared with subsurface samples (10–20, 20–30, and 30–40 cm) to evaluate the isotopic distribution and source of *n*-alkanes both laterally and vertically at various sites.

Sites 1, 2, 2a, and 3 have δ^{13}C *n*-alkane values which vary between −30.0 and −28.0‰. The profiles are generally flat, although minor fluctuations are observed, especially in the subsurface samples (Fig. 3a, b, c, and d) which consisted of a slight odd-predominance for *n*-alkanes higher than nC_{25}. Surface samples (0–10 cm) from Sites 1, 2, 2a, and 3 are heavier isotopically (between −28.0 and −29.0‰) than the deeper samples, which are up to 2.0‰ lighter.

A contaminated industrial petroleum area that had recently started bioremediation (breakdown of hydrocarbons using fertilizers) was sampled near Site 2a. Isotopic analysis of the sample was only possible between nC_{11} and nC_{17} due to sufficient biodegradation of alkanes between nC_{17} and nC_{33} (Fig. 3c; Table 5). The contaminated sediment contains heavier δ^{13}C values (between −28.2 and −25.8‰) than any other site in this study. Isotopic comparison of the contaminated sample and two nearby shore samples at Site 2a (Fig. 3c) showed a similar isotopic profile to one of the samples and bunker fuel.

Sites 4 and 5 showed lighter δ^{13}C values (between −31.3 and −28.5‰) than Sites 1, 2, and 3. Site 4, located on the north shore at the extreme east of the study area, had isotopic values between −31.3 and −30.4‰ (Fig. 3d) which are the lightest found in the study. The surface sample (0–10 cm) from Site 4 was slightly heavier isotopically than the subsurface sample (10–20 cm), following the trend previously seen in other sites. In both Sites 4 and 5, a slight odd-predominance was seen for the higher molecular weight *n*-alkanes. Site 5, located to the west of the study area, was more similar to samples from Sites 1, 2, and 3 for the lower weight homologues (up to C_{22}), with values between −29.4 and −28.7‰ (Fig. 3d).

However, for the higher homologues, the isotopic profile followed a similar pattern to those located at Site 4 with δ^{13}C values between −31.1 and −29.7‰. The isotopic profile of bunker fuel was generally flat and ranged between −28.8 and −27.6‰.

In summary, the main features documented include:

1. higher organic contents near petroleum storage sites in central Quebec City relative to beaches located further from the city;
2. lateral and vertical trends of $CPI_{15–21}$ and $CPI_{25–33}$ forming a spatial distribution pattern in which Sites 1, 2, and 3 are distinctly different from the other sites;
3. biomarker evidence from steranes and triterpanes support the *n*-alkane maturity trends; sterane patterns of all sites show similar C_{27}, C_{28}, C_{29}, and C_{30} patterns; and

Table 4
Sterane biomarker ratios

Sample	$C_{27}\alpha\alpha\alpha S$ S + R	%ββ C_{27}	$C_{29}\alpha\alpha S$ S + R	%ββ C_{29}	$C_{27}\alpha\alpha\alpha R$ $C_{29}\alpha\alpha\alpha R$	$C_{28}\alpha\alpha\alpha R$ $C_{29}\alpha\alpha\alpha R$	$C_{29}\alpha\beta\beta R$ $C_{29}\alpha\alpha\alpha R$	27βαS + RDia $C_{29}\alpha\alpha\alpha S + R$	%C_{27} steranes	%C_{28} steranes	%C_{29} steranes	%C_{30} steranes
Site 1 (0–10 cm)	0.41	0.37	0.57	0.53	1.19	0.79	1.33	0.63	38.3	25.4	32.1	4.2
Site 2a (0–10 cm)	0.62	0.42	0.67	0.58	1.00	0.73	2.08	3.06	33.2	24.1	33.2	9.4
Site 2 (0–10 cm)	0.49	0.34	0.57	0.53	1.42	0.80	1.23	0.40	42.2	23.8	29.7	4.3
Site 3 (0–10 cm)	0.41	0.31	0.53	0.55	0.82	0.62	1.05	0.36	31.1	23.6	38.0	7.3
Site 4 (0–10 cm)	0.60	0.33	0.48	0.51	0.41	0.52	0.84	0.49	19.9	25.7	49.1	5.2
Site 5 (0–10 cm)	0.43	0.36	0.56	0.55	1.58	0.55	1.36	1.78	47.5	16.6	30.0	5.9
Bunker fuel	0.44	0.46	0.53	0.58	1.62	0.30	1.34	1.02	51.6	9.6	31.9	7.0

Table 5
$\delta^{13}C$ values of individual *n*-alkanes from Sites 1, 2, 2a, 3, 4, and 5 with bunker fuel for comparison

Site	Depth (cm)	C_{11}	C_{12}	C_{13}	C_{14}	C_{15}	C_{16}	C_{17}	C_{18}	C_{19}	C_{20}	C_{21}	C_{22}	C_{23}	C_{24}	C_{25}	C_{26}	C_{27}	C_{28}	C_{29}	C_{30}	C_{31}
1	0–10	nd[a]	nd	nd	nd	−28.6	−28.6	−29.1	−28.6	−28.9	−28.9	−29.1	−29.0	−29.2	−28.1	−28.6	−28.6	−28.8	−28.4	−28.8	nd	nd
	0–10	nd	nd	nd	nd	−28.8	−28.3	−28.7	−28.7	−28.4	−28.5	−28.3	−28.5	−28.3	−28.5	−28.5	−28.2	−28.3	−28.4	−28.4	−28.6	nd
	0–20	nd	nd	nd	nd	nd	−29.4	−29.5	−29.3	−29.3	−29.4	−29.3	−29.4	−29.4	−29.6	−29.0	−29.2	−29.3	−29.2	−29.3	−29.0	−29.0
	20–30	nd	nd	nd	nd	−29.6	−29.6	−29.4	−29.5	−29.5	−29.9	−29.7	−30.1	−29.6	−29.5	−29.5	−29.4	−29.1	nd	nd	nd	nd
	30–40	nd	nd	nd	nd	−29.6	−29.6	−29.9	−29.7	−29.6	−29.8	−29.7	−29.5	−29.7	−29.5	−29.7	−29.2	−29.6	−29.5	−29.9	−29.3	−29.6
2	0–10	nd	nd	nd	nd	−28.1	−28.2	−28.5	−28.5	−28.6	−28.7	−28.9	−28.9	−28.9	−28.7	−28.7	−28.5	−28.6	−28.5	−28.7	nd	nd
	0–10	nd	nd	nd	nd	−28.2	−28.3	−28.4	−28.7	−28.7	−28.7	−28.8	−28.8	−28.7	−28.9	−29.0	−28.3	−28.7	−28.5	−28.7	nd	nd
	10–20	nd	nd	nd	nd	−28.2	−28.9	−29.2	−29.3	−29.4	−29.4	−29.6	−29.6	−29.5	−29.4	−29.2	−28.8	−28.0	−28.7	−29.2	−28.9	nd
	30–40	nd	nd	nd	nd	−29.3	−29.1	−29.0	−29.1	−29.2	−29.5	−29.7	−29.6	−29.4	−29.2	−29.2	−29.3	−29.1	nd	nd	nd	nd
2a	Contaminated	−27.0	−26.7	−25.8	−26.9	−27.7	−27.7	−28.2	nd	nd	nd	nd	nd	nd	nd	nd	nd	nd	nd	nd	nd	nd
	0–10	nd	nd	−29.7	−29.3	−29.3	−29.0	−29.2	−28.7	−28.8	−27.6	−28.9	−28.7	−28.5	−28.5	−28.4	−28.5	−28.8	−28.7	−29.2	−28.9	−29.4
	0–10	nd	−25.7	−25.4	−27.4	−27.7	−27.9	−28.1	−28.0	−28.1	−28.1	−28.3	−28.5	−28.5	−28.6	−28.9	−28.8	−28.8	−28.8	−29.1	−28.7	−29.6
3	0–10	nd	−29.3	−28.0	−28.3	−28.5	−28.5	−28.8	−28.3	−27.4	−28.1	−27.6	−27.8	−28.3	−28.2	−27.8	−28.2	−28.6	−28.3	−28.8	−28.5	−29.0
	0–10	nd	nd	nd	nd	−29.6	−29.1	−29.0	−29.0	−28.2	−28.4	−28.2	−28.4	−28.2	−27.7	−28.0	−28.0	−28.3	−29.1	−29.2	−28.5	nd
	30–40	nd	nd	nd	nd	−29.8	−29.9	−29.7	−29.9	−29.8	−29.9	−29.9	−29.5	−29.4	−29.3	−29.5	−29.3	−29.4	−29.5	−29.7	−29.4	nd
4	0–10	nd	nd	nd	nd	−30.5	−30.4	−30.5	−30.7	−30.5	−30.6	−30.6	−30.7	−30.5	−30.5	−30.4	−30.5	−30.5	−30.4	−30.6	−30.5	nd
	10–20	nd	nd	nd	nd	−31.0	−31.2	−31.3	−31.1	−31.0	−31.1	−31.1	−31.1	−30.9	−30.8	−30.9	−30.8	−30.8	−30.6	−30.8	−30.6	nd
5	0–10	nd	nd	nd	nd	−28.7	−28.9	−28.9	−29.2	−29.1	−29.1	−29.4	−29.4	−29.7	−30.1	−30.0	−29.7	−30.2	−30.3	−30.9	−30.7	nd
Bunker fuel		nd	nd	nd	−28.0	−28.0	−28.1	−27.9	−27.6	−27.9	−27.7	−27.9	−28.0	−27.9	−27.9	−28.2	−28.6	−28.7	−28.8	−28.7	−28.6	−28.8

[a] nd = not detected.

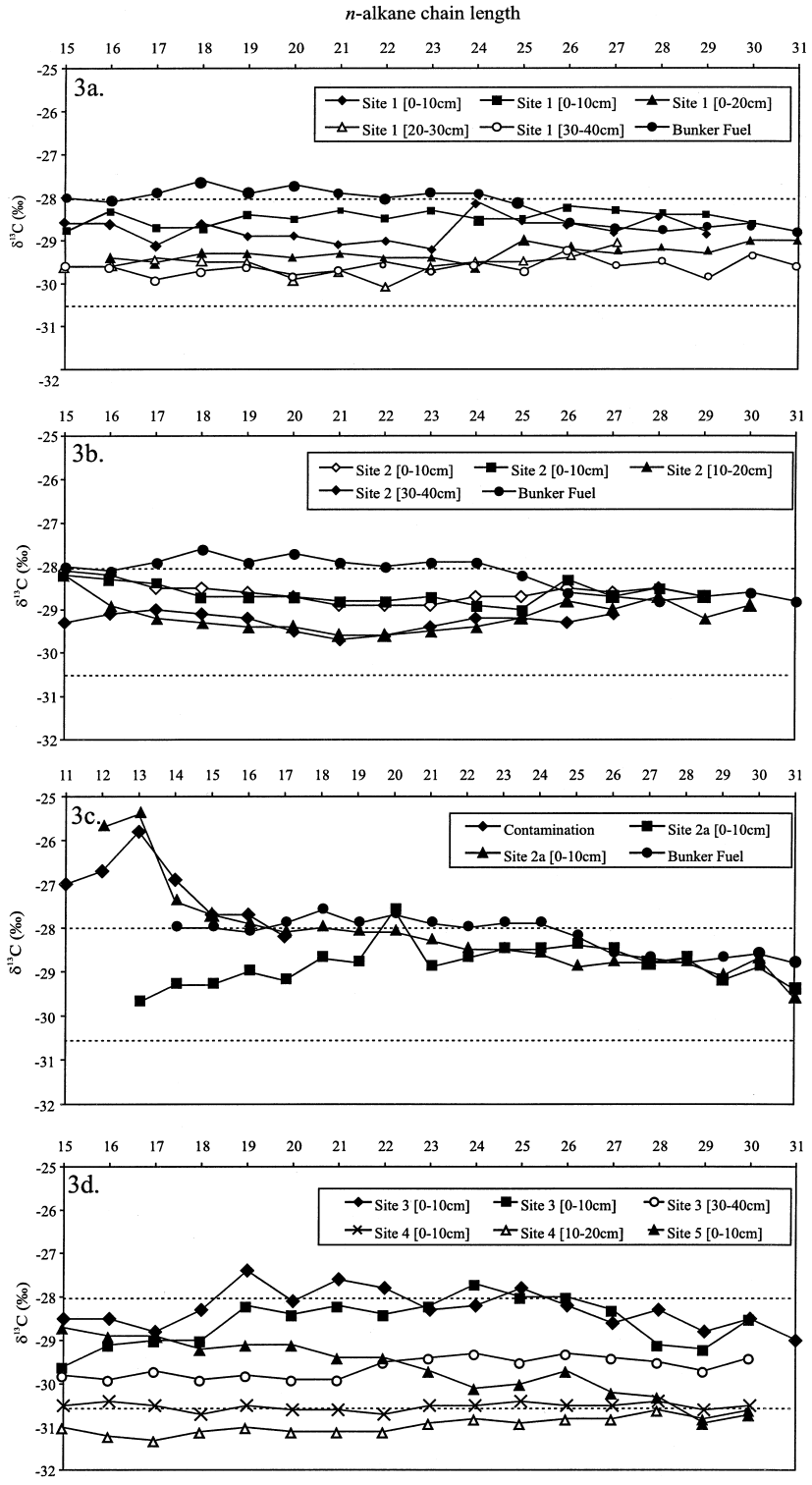

Fig. 3. Individual *n*-alkane carbon isotopic values of: (3a) Site 1 with bunker fuel for comparison; (3b) Site 2 with bunker fuel for comparison; (3c) Site 2a and a classified contaminated site with bunker fuel for comparison; and (3d) Sites 3, 4 and 5.

4. the contaminated sample and bunker fuel show the heaviest $\delta^{13}C$ values while sites located further away from the city contain lighter $\delta^{13}C$ values; in general the isotopic profiles are flat, although a slight odd–even predominance is noted in higher homologues for samples located further away from the city and for deeper samples.

4. Discussion

Some beach sands located along the St Lawrence River near Quebec City contain uncommonly high organic contents and unusual *n*-alkane profiles usually associated with older fine-grained sediments rather than recent surface sands. These surface sands also have unimodal *n*-alkane distributions with a maximum around nC_{15} or nC_{17}, and a low odd–even predominance, typically associated with a marine sourced oil. Organic pyrolysis indicates that surface sands from St Lawrence River beaches adjacent to Quebec City (Sites 1, 2, and 3) contain the highest organic carbon content. Surface samples located further away from the central region at Sites 4 and 5 contain slightly higher CPI values suggesting a mixture of indigenous and anthropogenic inputs.

In general, subsurface samples contain lower organic levels than surface counterparts, and display unimodal or bimodal *n*-alkane distributions around nC_{15} or nC_{29}, with higher CPI values. Both $CPI_{15–21}$ and $CPI_{25–31}$ values increase from surface to subsurface samples suggesting surface sediments are more mature than subsurface sediments (Table 2). This vertical trend was seen predominantly near Sites 1, 2, 2a, and 3 located centrally around Quebec City. Sites 4 and 5, located further away from the city, had higher overall CPI values in both surface and especially subsurface sediments than those samples from the central region. An increase in the subsurface $CPI_{25–31}$ values relative to the surface $CPI_{25–31}$ values reflects higher plant contributions, and suggests increasing indigenous combined with decreasing anthropogenic organic input. Collectively, these data suggest surface dispersal of an anthropogenic source as the primary source of contamination rather than subsurface leakage.

Slight biodegradation is suggested for the surface samples from the central Quebec City region (Sites 1, 2, and 3) based on their higher abundance of isoprenoids relative to *n*-alkanes. Surface samples (0–10 cm) have pristane and phytane concentrations usually exceeding those of the corresponding C_{17} and C_{18} *n*-alkanes, suggesting slight to mild biodegradation. Pr/nC_{17} ratios suggest that bacterial attack and biodegradation is preferentially taking place at the surface, as deeper samples have much lower ratios. Samples from Sites 4 and 5 show little evidence of biodegradation as indicated by low isoprenoid to *n*-alkane abundance.

GC–MS confirmed the presence of an anthropogenic input on the basis of mature biomarker (triterpane and sterane) distributions, which is not consistent with organic matter from recent sediments. Furthermore, they support the presence of an oil derived from marine organic matter based on the abundant C_{27} and C_{29} regular and rearranged steranes and a minor C_{30} sterane contribution (Peters et al., 1986).

Higher C_{27} and C_{29} diasterane levels such as those found in mature samples located at Quebec City may reflect the slight biodegradation already observed in some samples, as steranes are preferentially degraded before diasteranes (Peters and Moldowan, 1993). This could give some anomalous values as in Sample 8 (the only sample to have all the *n*-alkanes removed by biodegradation) and enhance the C_{27} and C_{29} diasteranes relative to regular steranes.

Biomarker comparisons with the bunker fuel show similarities to samples from Sites 1, 2, and 3, suggesting an oil-contamination correlation. The sterane fingerprint of the bunker fuel shows similar characteristics to the beach sands and contains high C_{27} diasteranes combined with high C_{27} and C_{29} regular steranes and smaller abundance of C_{30} steranes. The maturity data for the $\%\beta\beta C_{27}$ and $\%\beta\beta C_{29}$ steranes shows that the bunker fuel and beach sand samples display similar levels of maturity. The $C_{29}\alpha\alpha\alpha$ S/S + R ratio (peaks 5 and 8) of Sites 1, 2, and 3 also match the bunker fuel trends, as do the C_{30} steranes. In contrast, Site 4 shows a slightly lower maturity than the other sites from the central region. GC–IRMS *n*-alkane profiles also show a corresponding trend whereby surface samples from Sites 1, 2a, and 3 correlate closely with the bunker fuel.

Analyses of individual *n*-alkanes from surface samples located from Sites 1, 2, 2a, and 3 generally show flat isotopic profiles, with values between −30.0 and −28.0‰. In general, all surface samples from Sites 1, 2, and 3 show an isotopic profile similar to the bunker fuel, consisting of a flat profile which drops gradually by 0.5‰ to 1.0‰ at nC_{25}. These values lie in the isotopic range given for the analysed bunker fuel sample (Fig. 3a, b, and c) and some petroleum products (Uzaki et al., 1993; Ishiwatari et al., 1994), supporting GC and GC–MS results of a mature anthropogenic contribution. Low isotopic variation between odd- and even-numbered carbon *n*-alkanes suggests these *n*-alkanes are predominantly derived from one source, rather than an indigenous and anthropogenic mixture. Subsurface samples from the same location display isotopically lighter $\delta^{13}C$ values (up to 2‰) than their surface counterparts with slight odd-predominance for the higher molecular weight homologues ($< nC_{25}$). This probably suggests a combination of an anthropogenic source with a small indigenous terrestrial contribution.

The $\delta^{13}C$ values of *n*-alkanes from the contaminated sample near Site 2a are enriched relative to other samples

from this study, which could be due to the effects of biodegradation. One of the two samples from Site 2a correlate well with the sample from the contaminated area, but shows a odd-predominance between nC_{25} and nC_{31}. This correlation suggests that the samples could be related, although there is insufficient evidence to suggest that the contaminated site is leaking hydrocarbons into the river. Tidal dispersion, water washing, or groundwater circulation may be responsible for transporting similar anthropogenic material from other sites, rather than leakage onto the shore. A complete isotopic profile of the contamination was not possible because of the removal of *n*-alkanes.

Site 4 contains the lowest $\delta^{13}C$ values from this study, which suggests that the influence of an anthropogenic contribution is lower than at other sites. The $\delta^{13}C$ values (-31.3 to -30.4‰) of Site 4 are at the limit of the traditional region for petroleum hydrocarbons suggesting that an indigenous contribution may be responsible for the isotopic depletion. This is also supported by the higher CPI values previously observed using GC. The surface sample is isotopically heavier than the deeper sample (10–20 cm) suggesting that some anthropogenic contribution may have contributed to the source organic material.

An isotopic profile of a surface sample from Site 5 shows heavier $\delta^{13}C$ values between C_{15} and C_{23}, then lighter values between C_{25} and C_{31}. This suggests a slightly greater anthropogenic input than Site 4, isotopically enriching the lower molecular weight *n*-alkanes.

A previous study by Ishiwatari et al. (1994) of some oil-polluted sediments in Tokyo Bay found fine-grained surface sediments which contained odd-numbered *n*-alkanes lighter isotopically than the even-numbered *n*-alkanes. Ishiwatari et al. (1994) attributed this to mixing of indigenous and of petroleum-related *n*-alkanes. In this study these variations were rarely seen except in some subsurface samples because coarser-grained sediments do not retain the indigenous signature as easily as fine-grained sediments. A similar pattern was noted in some samples, predominantly in higher molecular weight homologues, suggesting that the main indigenous contribution consists of higher plant input giving rise to odd higher molecular weight alkanes.

Surface samples farther from industrial areas usually showed isotopic profiles similar to those previously seen in contaminated samples (Sites 1, 2, 2a, and 3), but the $\delta^{13}C$ values were lighter than those surface and subsurface samples. Gas chromatograms of these samples showed none of the characteristic features of biodegradation (*n*-alkane depletion, enhanced isoprenoids relative to *n*-alkanes, large unresolved humps), although some odd–even predominance was seen in most samples, and for the higher molecular weight homologues. Therefore, mixing and dilution of anthropogenic sources by indigenous organic matter is suggested as the main processes accounting for the observed distributions.

5. Conclusions

The most likely source of the contamination has been shown using GC, GC–MS, and GC–IRMS to be bunker fuel, or an oil which contains very similar properties (a fuel used as boiler fuel in ships, commercial, or industrial heating). Triterpane, sterane and *n*-alkane chromatograms show similar fingerprints between bunker fuel and the organic extracts from most beach sands located in the central Quebec City region. Variations in biomarker maturity parameters are largely related to varying amounts of petroleum products contaminating the sediments. In all cases except the contaminated site, the isotopic profile of the bunker fuel has a slightly heavier isotopic signature than the surface sediments that were sampled. This is consistent with an anthropogenic source combined with varying amounts of indigenous organic matter resulting in a lighter isotopic signature.

At this stage, no conclusive evidence can be shown for leakage or contamination from any particular site, although isotopic similarities exist between a known contaminated site and the nearby shore sediments. The contaminated site also shows a strong isotopic correlation to bunker fuel, and therefore the transfer of bunker fuel from shore to ship is suggested as the most likely source of pollution with a wide dispersal area due to the tidal nature of the river. In general, the distribution of petroleum pollutants along the river shore appears to be most concentrated in the region surrounding Sites 1, 2, 2a, and 3.

This study has shown that samples that contain heavier $\delta^{13}C$ values have higher levels of anthropogenic components, suggesting the contaminant has $\delta^{13}C$ values between -29.0 and -28.0‰. The anthropogenic signature decreases away from Sites 1, 2, and 3, suggested by isotopically lighter $\delta^{13}C$ values seen in Sites 4 and 5, and by lighter subsurface isotopic values in the central region. Site 4 has the lightest isotopic values in the study and is located in the far southwest of the study area. The effects of river current on anthropogenic transport can therefore be seen using GC–IRMS. Our results suggest that river currents transport the contamination from the central Quebec City region (Sites 1, 2, and 3) predominantly towards the east (Site 5).

GC–IRMS data suggest the presence of a marine oil around central Quebec City region based on the carbon isotopic values of *n*-alkanes between -30.0 and -28.0‰ and biomarker data. Less contaminated areas suggest mixing of indigenous terrestrial and anthropogenic material, shown by correspondingly light $\delta^{13}C$ values. The effects of biodegradation were low, except for Sample 8 which had the *n*-alkanes totally removed. However, biodegradation of hydrocarbons at a site undergoing bacterial bioremediation using fertilizers resulted in heavier isotopic values than other samples.

Associate Editor—**A.G. Requejo**

Acknowledgements

The authors are grateful to Marc Luzincourt (CGQ), Biogénie Inc., and the Ministère de l'Environnement et de la faune du Québec for use of their GC–MS. GSC contribution number 1998011. We would also like to thank Drs. Vincent O'Malley, James Collister, and Rick Requejo for helpful comments and reviews.

References

Bjorøy, M., Hall, P.B., Moe, R.P., 1994. Variation in the isotopic composition of single components in the C_4–C_{20} fraction of oils and condensates. Organic Geochemistry 21, 761–776.

Blumer, M., Guillard, R.R., Chase, T., 1971. Hydrocarbons of marine phytoplankton. International Journal of Life in Oceans, Coastal Waters 8, 180–183.

Boreham, C.J., Summons, R.E., Roksandic, Z., Dowling, L.M., Hutton, A.C., 1994. Chemical, molecular and isotopic differentiation of organic facies in the Tertiary lacustrine Duaringa oil shale deposit, Queensland, Australia. Organic Geochemistry 21, 685–712.

Clark Jr., R.C., Blumer, M., 1967. Distribution of *n*-parrafins in marine organisms and sediment. Limnology and Oceanography 12, 79–87.

Collister, J.W., Lichtfouse, E., Hieshima, G., Hayes, J.M., 1994. Partial resolution of sources of *n*-alkanes in the saline portion of the Parachute Creek Member, Green River Formation (Piceance Creek Basin, Colorado). Organic Geochemistry 21, 645–659.

Eglinton, G., Gonzales, A.G., Hamilton, R.J., Raphael, R.A., 1962. Hydrocarbon constituents of the wax coatings of plant leaves: a taxonomic survey. Phytochemistry 1, 89–102.

Gelpi, E., Oro, J., Schneider, H.J., Bennett, E.O., 1970. Hydrocarbons of geochemical significance in microscopic algae. Phytochemistry 9, 603–612.

Harada, N., Handa, N., Fukuchi, M., Ishiwatari, R., 1995. Source of hydrocarbons in marine sediments in Lützow-Holm Bay, Antarctica. Organic Geochemistry 23, 229–237.

Hirner, A.V., Lyon, G.L., 1989. Stable isotope geochemistry of crude oils and of possible source rocks from New Zealand — 1: carbon. Applied Geochemistry 4, 109–120.

Ishiwatari, R., Uzaki, M., Yamada, K., 1994. Carbon isotope composition of individual *n*-alkanes in recent sediments. Organic Geochemistry 21, 801–808.

Kaplan, I.R., Galperin, Y., Alimi, H., Lee, R., Lu, S., 1996. Patterns of chemical changes during environmental alteration of hydrocarbon fuels. Ground Water Monitoring and Remediation Fall, 113–124.

Lichtfouse, E., Derenne, S., Mariotti, A., Largeau, C., 1994. Possible algal origin of long chain odd *n*-alkanes in immature sediments as revealed by distribution and carbon isotope ratios. Organic Geochemistry 22, 1023–1027.

Mansuy, L., Philp, R.P., Allen, J., Kombrink, M., 1996. GC–IRMS as a potential tool for the determination of the source of hydrocarbons in contaminated soils and waters. In: Crelling, J.C. (Ed.), Thirteenth Annual Meeting of the Society for Organic Petrology, Abstracts and Program.

Peters, K.E., Moldowan, J.M., 1993. The Biomarker Guide: Interpreting Molecular Fossils in Petroleum and Ancient Sediments. Prentice-Hall, New Jersey.

Peters, K.E., Moldowan, J.M., Schoell, J.M., Hempkins, W.B., 1986. Petroleum isotopic and biomarker composition related to source rock organic matter and depositional environment. Organic Geochemistry 10, 17–27.

Rieley, G., Collier, R.J., Jones, D.M., Eglinton, G., Eakin, P.A., Fallick, A.E., 1991. Sources of sedimentary lipids deduced from stable carbon-isotope analyses of individual compounds. Nature 352, 425–427.

Simoneit, B.R.T., 1978. The organic chemistry of marine sediments. In: Reily, J.P., Chester, R. (Eds.), Chemical Oceanography, Vol. 7, Chapter 390. Academic Press, London, pp. 233–311.

Sofer, Z., Bjorøy, M., Hustad, E., 1991. Isotopic composition of individual *n*-alkanes in oils. In: Manning, D.A.C. (Ed.), Organic Geochemistry — Advances and Applications in Energy and the Natural Environment. Manchester University Press, Manchester, pp. 207–211.

Uzaki, M., Yamada, K., Ishiwatari, R., 1993. Carbon isotope evidence for oil-pollution in long chain normal alkanes in Tokyo Bay sediments. Geochemical Journal 27, 385–389.

Volkman, J.K., 1984. Biodegredation of aromatic hydrocarbons in crude oils from the Barrow sub-basin of Western Australia. Organic Geochemistry 6, 619–632.